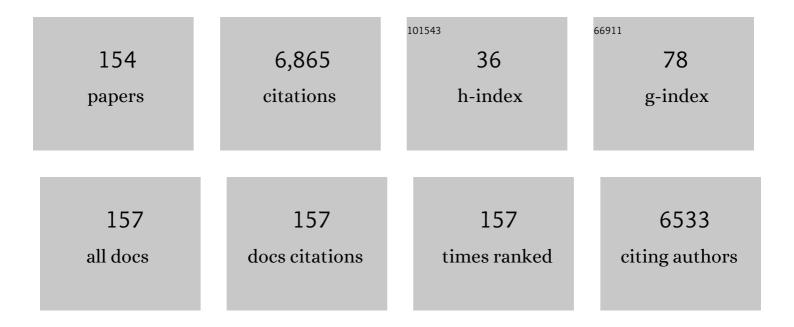
Patrick P Mercier

List of Publications by Year in descending order

Source: https://exaly.com/author-pdf/7893501/publications.pdf Version: 2024-02-01



#	Article	IF	CITATIONS
1	A wearable chemical–electrophysiological hybrid biosensing system for real-time health and fitness monitoring. Nature Communications, 2016, 7, 11650.	12.8	639
2	Wearable salivary uric acid mouthguard biosensor with integrated wireless electronics. Biosensors and Bioelectronics, 2015, 74, 1061-1068.	10.1	471
3	Noninvasive Alcohol Monitoring Using a Wearable Tattoo-Based Iontophoretic-Biosensing System. ACS Sensors, 2016, 1, 1011-1019.	7.8	460
4	Simultaneous Monitoring of Sweat and Interstitial Fluid Using a Single Wearable Biosensor Platform. Advanced Science, 2018, 5, 1800880.	11.2	371
5	Soft, stretchable, high power density electronic skin-based biofuel cells for scavenging energy from human sweat. Energy and Environmental Science, 2017, 10, 1581-1589.	30.8	309
6	Non-invasive mouthguard biosensor for continuous salivary monitoring of metabolites. Analyst, The, 2014, 139, 1632-1636.	3.5	292
7	Eyeglasses based wireless electrolyte and metabolite sensor platform. Lab on A Chip, 2017, 17, 1834-1842.	6.0	211
8	An integrated wearable microneedle array for the continuous monitoring of multiple biomarkers in interstitial fluid. Nature Biomedical Engineering, 2022, 6, 1214-1224.	22.5	186
9	Energy extraction from the biologic battery in the inner ear. Nature Biotechnology, 2012, 30, 1240-1243.	17.5	183
10	Design and Analysis of a Three-Phase Wireless Charging System for Lightweight Autonomous Underwater Vehicles. IEEE Transactions on Power Electronics, 2018, 33, 6622-6632.	7.9	162
11	Wearable textile biofuel cells for powering electronics. Journal of Materials Chemistry A, 2014, 2, 18184-18189.	10.3	156
12	Microneedle-Based Detection of Ketone Bodies along with Glucose and Lactate: Toward Real-Time Continuous Interstitial Fluid Monitoring of Diabetic Ketosis and Ketoacidosis. Analytical Chemistry, 2020, 92, 2291-2300.	6.5	154
13	A 1.1 nW Energy-Harvesting System with 544 pW Quiescent Power for Next-Generation Implants. IEEE Journal of Solid-State Circuits, 2014, 49, 2812-2824.	5.4	131
14	An Energy-Efficient All-Digital UWB Transmitter Employing Dual Capacitively-Coupled Pulse-Shaping Drivers. IEEE Journal of Solid-State Circuits, 2009, 44, 1679-1688.	5.4	112
15	A Pulsed UWB Receiver SoC for Insect Motion Control. IEEE Journal of Solid-State Circuits, 2010, 45, 153-166.	5.4	109
16	A Near-Zero-Power Wake-Up Receiver Achieving â^'69-dBm Sensitivity. IEEE Journal of Solid-State Circuits, 2018, 53, 1640-1652.	5.4	101
17	Integrated Coil Design for EV Wireless Charging Systems Using <i>LCC</i> Compensation Topology. IEEE Transactions on Power Electronics, 2018, 33, 9231-9241.	7.9	93
18	Re-usable electrochemical glucose sensors integrated into a smartphone platform. Biosensors and Bioelectronics, 2018, 101, 181-187.	10.1	93

#	Article	IF	CITATIONS
19	A Recursive Switched-Capacitor DC-DC Converter Achieving <formula formulatype="inline"><tex notation="TeX">\$2^{N}-1\$</tex> Ratios With High Efficiency Over a Wide Output Voltage Range. IEEE Journal of Solid-State Circuits, 2014, 49, 2773-2787.</formula 	5.4	87
20	Neural recording and stimulation using wireless networks of microimplants. Nature Electronics, 2021, 4, 604-614.	26.0	81
21	A Sub-nW 2.4 GHz Transmitter for Low Data-Rate Sensing Applications. IEEE Journal of Solid-State Circuits, 2014, 49, 1463-1474.	5.4	79
22	MISIMO: A Multi-Input Single-Inductor Multi-Output Energy Harvesting Platform in 28-nm FDSOI for Powering Net-Zero-Energy Systems. IEEE Journal of Solid-State Circuits, 2018, 53, 3407-3419.	5.4	74
23	Channel Modeling of Miniaturized Battery-Powered Capacitive Human Body Communication Systems. IEEE Transactions on Biomedical Engineering, 2017, 64, 452-462.	4.2	72
24	A Rotation-Resilient Wireless Charging System for Lightweight Autonomous Underwater Vehicles. IEEE Transactions on Vehicular Technology, 2018, 67, 6935-6942.	6.3	71
25	Low-Power Impulse UWB Architectures and Circuits. Proceedings of the IEEE, 2009, 97, 332-352.	21.3	70
26	Wireless Power Transfer with Concurrent 200 kHz and 6.78 MHz Operation in a Single Transmitter Device. IEEE Transactions on Power Electronics, 2015, , 1-1.	7.9	68
27	Silicon-Integrated High-Density Electrocortical Interfaces. Proceedings of the IEEE, 2017, 105, 11-33.	21.3	68
28	A 144-MHz Fully Integrated Resonant Regulating Rectifier With Hybrid Pulse Modulation for mm-Sized Implants. IEEE Journal of Solid-State Circuits, 2017, 52, 3043-3055.	5.4	67
29	A Successive Approximation Recursive Digital Low-Dropout Voltage Regulator With PD Compensation and Sub-LSB Duty Control. IEEE Journal of Solid-State Circuits, 2018, 53, 35-49.	5.4	58
30	A 0.3-V CMOS Biofuel-Cell-Powered Wireless Glucose/Lactate Biosensing System. IEEE Journal of Solid-State Circuits, 2018, 53, 3126-3139.	5.4	55
31	The Language of Glove: Wireless gesture decoder with low-power and stretchable hybrid electronics. PLoS ONE, 2017, 12, e0179766.	2.5	55
32	A 6.1-nW Wake-Up Receiver Achieving â^'80.5-dBm Sensitivity Via a Passive Pseudo-Balun Envelope Detector. IEEE Solid-State Circuits Letters, 2018, 1, 134-137.	2.0	52
33	Rapid Wireless Capacitor Charging Using a Multi-Tapped Inductively-Coupled Secondary Coil. IEEE Transactions on Circuits and Systems I: Regular Papers, 2013, 60, 2263-2272.	5.4	48
34	A 0.4-V 0.93-nW/kHz Relaxation Oscillator Exploiting Comparator Temperature-Dependent Delay to Achieve 94-ppm/°C Stability. IEEE Journal of Solid-State Circuits, 2018, 53, 3004-3011.	5.4	47
35	A 2.4 GHz Multi-Channel FBAR-based Transmitter With an Integrated Pulse-Shaping Power Amplifier. IEEE Journal of Solid-State Circuits, 2013, 48, 1042-1054.	5.4	41

#	Article	IF	CITATIONS
37	Metallic Nanoislands on Graphene for Monitoring Swallowing Activity in Head and Neck Cancer Patients. ACS Nano, 2018, 12, 5913-5922.	14.6	38
38	A Reference-Free Capacitive-Discharging Oscillator Architecture Consuming 44.4 pW/75.6 nW at 2.8 Hz/6.4 kHz. IEEE Journal of Solid-State Circuits, 2016, 51, 1423-1435.	5.4	36
39	A 0.6V 75nW All-CMOS Temperature Sensor With 1.67m°C/mV Supply Sensitivity. IEEE Transactions on Circuits and Systems I: Regular Papers, 2017, 64, 2274-2283.	5.4	34
40	A 3 mm × 3 mm Fully Integrated Wireless Power Receiver and Neural Interface System-on-Chip. IEEE Transactions on Biomedical Circuits and Systems, 2019, 13, 1736-1746.	4.0	34
41	20.3 A 100nA-to-2mA successive-approximation digital LDO with PD compensation and sub-LSB duty control achieving a 15.1ns response time at 0.5V. , 2017, , .		33
42	A 3.4-pW 0.4-V 469.3 ppm/°C Five-Transistor Current Reference Generator. IEEE Solid-State Circuits Letters, 2018, 1, 122-125.	2.0	33
43	A 0.01-mm ² Mostly Digital Capacitor-Less AFE for Distributed Autonomous Neural Sensor Nodes. IEEE Solid-State Circuits Letters, 2018, 1, 162-165.	2.0	32
44	A 14.5 pW, 31 ppm/°C resistor-less 5 pA current reference employing a self-regulated push-pull voltage reference generator. , 2016, , .		31
45	Near-Zero-Power Temperature Sensing via Tunneling Currents Through Complementary Metal-Oxide-Semiconductor Transistors. Scientific Reports, 2017, 7, 4427.	3.3	31
46	A Fully Integrated Li-Ion-Compatible Hybrid Four-Level DC–DC Converter in 28-nm FDSOI. IEEE Journal of Solid-State Circuits, 2019, 54, 720-732.	5.4	31
47	A 22.3-nW, 4.55 cm ² Temperature-Robust Wake-Up Receiver Achieving a Sensitivity of â^69.5 dBm at 9 GHz. IEEE Journal of Solid-State Circuits, 2020, 55, 1530-1541.	5.4	30
48	A battery-connected 24-ratio switched capacitor PMIC achieving 95.5%-efficiency. , 2015, , .		29
49	MISIMO: A multi-input single-inductor multi-output energy harvester employing event-driven MPPT control to achieve 89% peak efficiency and a 60,000x dynamic range in 28nm FDSOI. , 2018, , .		29
50	Energy Efficient Pulsed-UWB CMOS Circuits and Systems. , 2007, , .		28
51	Balloonâ€Embedded Sensors Withstanding Extreme Multiaxial Stretching and Global Bending Mechanical Stress: Towards Environmental and Security Monitoring. Advanced Materials Technologies, 2016, 1, 1600061.	5.8	28
52	A 400 MHz 4.5 nW â^'63.8 dBm sensitivity wake-up receiver employing an active pseudo-balun envelope detector. , 2017, , .		28
53	Ultra-low-power UWB for sensor network applications. , 2008, , .		26
54	A pulsed UWB receiver SoC for insect motion control. , 2009, , .		26

4

#	Article	IF	CITATIONS
55	A Dynamically High-Impedance Charge-Pump-Based LDO With Digital-LDO-Like Properties Achieving a Sub-4-fs FoM. IEEE Journal of Solid-State Circuits, 2020, 55, 719-730.	5.4	26
56	23.2 A 1.1nW energy harvesting system with 544pW quiescent power for next-generation implants. , 2014, , .		25
57	A Sub-10-pJ/bit 5-Mb/s Magnetic Human Body Communication Transceiver. IEEE Journal of Solid-State Circuits, 2019, 54, 3031-3042.	5.4	25
58	A Low-Voltage Energy-Sampling IR-UWB Digital Baseband Employing Quadratic Correlation. IEEE Journal of Solid-State Circuits, 2010, 45, 1209-1219.	5.4	24
59	A Current-Mode Capacitively-Coupled Chopper Instrumentation Amplifier for Biopotential Recording With Resistive or Capacitive Electrodes. IEEE Transactions on Circuits and Systems II: Express Briefs, 2018, 65, 699-703.	3.0	24
60	A 93% Peak Efficiency Fully-Integrated Multilevel Multistate Hybrid DC–DC Converter. IEEE Transactions on Circuits and Systems I: Regular Papers, 2018, 65, 2617-2630.	5.4	23
61	A 763 pW 230 pJ/Conversion Fully Integrated CMOS Temperature-to-Digital Converter With +0.81 °C/â^°0.75 °C Inaccuracy. IEEE Journal of Solid-State Circuits, 2019, 54, 2281-2290.	5.4	23
62	A 112-dB SFDR 89-dB SNDR VCO-Based Sensor Front-End Enabled by Background-Calibrated Differential Pulse Code Modulation. IEEE Journal of Solid-State Circuits, 2021, 56, 1046-1057.	5.4	23
63	A Battery-Powered Wireless Ion Sensing System Consuming 5.5 nW of Average Power. IEEE Journal of Solid-State Circuits, 2018, 53, 2043-2053.	5.4	22
64	A 420 fW self-regulated 3T voltage reference generator achieving 0.47%/V line regulation from 0.4-to-1.2 V. , 2017, , .		21
65	Magnetic human body communication. , 2015, 2015, 1841-4.		20
66	A 1.6%/V 124.2 pW 9.3 Hz relaxation oscillator featuring a 49.7 pW voltage and current reference generator. , 2017, , .		20
67	An Interference-Resilient BLE-Compatible Wake-Up Receiver Employing Single-Die Multi-Channel FBAR-Based Filtering and a 4-D Wake-Up Signature. IEEE Journal of Solid-State Circuits, 2021, 56, 416-426.	5.4	20
68	A three-phase wireless charging system for lightweight autonomous underwater vehicles. , 2017, , .		19
69	A Fully Integrated RF-Powered Energy-Replenishing Current-Controlled Stimulator. IEEE Transactions on Biomedical Circuits and Systems, 2019, 13, 191-202.	4.0	18
70	A Sub-mW 2.4-GHz Active-Mixer-Adopted Sub-Sampling PLL Achieving an FoM of -256 dB. IEEE Journal of Solid-State Circuits, 2019, , 1-11.	5.4	17
71	Wireless powering of mm-scale fully-on-chip neural interfaces. , 2017, , .		16
72	Distributed Microscale Brain Implants with Wireless Power Transfer and Mbps Bi-directional Networked Communications. , 2019, , .		16

#	Article	IF	CITATIONS
73	Robust Biopotential Acquisition via a Distributed Multi-Channel FM-ADC. IEEE Transactions on Biomedical Circuits and Systems, 2019, 13, 1229-1242.	4.0	16
74	8.2 A Continuous-Input-Current Passive-Stacked Third-Order Buck Converter Achieving 0.7W/mm ² Power Density and 94% Peak Efficiency. , 2019, , .		16
75	A Symmetric Modified Multilevel Ladder PMIC for Battery-Connected Applications. IEEE Journal of Solid-State Circuits, 2020, 55, 767-780.	5.4	16
76	A Low-Power Backscatter Modulation System Communicating Across Tens of Meters With Standards-Compliant Wi-Fi Transceivers. IEEE Journal of Solid-State Circuits, 2020, 55, 2959-2969.	5.4	16
77	A Dual-Mode Wi-Fi/BLE Wake-Up Receiver. IEEE Journal of Solid-State Circuits, 2021, 56, 1288-1298.	5.4	16
78	Wearable chemical sensors: Opportunities and challenges. , 2016, , .		15
79	A fully integrated 144 MHz wireless-power-receiver-on-chip with an adaptive buck-boost regulating rectifier and low-loss H-Tree signal distribution. , 2016, , .		15
80	A Digitally Assisted Multiplexed Neural Recording System With Dynamic Electrode Offset Cancellation via an LMS Interference-Canceling Filter. IEEE Journal of Solid-State Circuits, 2022, 57, 953-964.	5.4	15
81	Channel Characterization of Magnetic Human Body Communication. IEEE Transactions on Biomedical Engineering, 2022, 69, 569-579.	4.2	14
82	A 19pJ/pulse UWB transmitter with dual capacitively-coupled digital power amplifiers. , 2008, , .		13
83	A 0.55V 16Mb/s 1.6mW non-coherent IR-UWB digital baseband with ±1ns synchronization accuracy. , 2009, , .		13
84	A 45-ratio recursively sliced series-parallel switched-capacitor DC-DC converter achieving 86% efficiency. , 2014, , .		13
85	Design of miniaturized wireless power receivers for mm-sized implants. , 2017, , .		13
86	A 178.9-dB FoM 128-dB SFDR VCO-Based AFE for ExG Readouts With a Calibration-Free Differential Pulse Code Modulation Technique. IEEE Journal of Solid-State Circuits, 2021, 56, 3236-3246.	5.4	13
87	A Supply-Rail-Coupled eTextiles Transceiver for Body-Area Networks. IEEE Journal of Solid-State Circuits, 2011, 46, 1284-1295.	5.4	12
88	Noise Analysis of Phase-Demodulating Receivers Employing Super-Regenerative Amplification. IEEE Transactions on Microwave Theory and Techniques, 2017, 65, 3299-3311.	4.6	12
89	A Passive-Stacked Third-Order Buck Converter With Inherent Input Filtering Achieving 0.7-W/mm\$^{2}\$ Power Density and 94% Peak Efficiency. IEEE Solid-State Circuits Letters, 2019, 2, 240-243.	2.0	12
90	A Wearable, Extensible, Open-Source Platform for Hearing Healthcare Research. IEEE Access, 2019, 7, 162083-162101.	4.2	12

#	Article	IF	CITATIONS
91	28.2 A 220μW -85dBm Sensitivity BLE-Compliant Wake-up Receiver Achieving -60dB SIR via Single-Die Multi- Channel FBAR-Based Filtering and a 4-Dimentional Wake-Up Signature. , 2019, , .		12
92	Epidermal Graphene Sensors and Machine Learning for Estimating Swallowed Volume. ACS Applied Nano Materials, 2021, 4, 8126-8134.	5.0	12
93	A 51 pW reference-free capacitive-discharging oscillator architecture operating at 2.8 Hz. , 2015, , .		11
94	A 0.6-mW 16-FSK Receiver Achieving a Sensitivity of â~'103 dBm at 100 kb/s. IEEE Journal of Solid-State Circuits, 2021, 56, 1299-1309.	5.4	11
95	A 1.2nW Analog Electrocardiogram Processor Achieving a 99.63% QRS Complex Detection Sensitivity. IEEE Transactions on Biomedical Circuits and Systems, 2021, 15, 617-628.	4.0	11
96	A miniaturized ultrasonic power delivery system. , 2014, , .		10
97	An Optically Addressed Nanowire-Based Retinal Prosthesis With Wireless Stimulation Waveform Control and Charge Telemetering. IEEE Journal of Solid-State Circuits, 2021, 56, 3263-3273.	5.4	10
98	A Stochastic Resonance Electrocardiogram Enhancement Algorithm for Robust QRS Detection. IEEE Journal of Biomedical and Health Informatics, 2022, 26, 3743-3754.	6.3	10
99	A 144MHz integrated resonant regulating rectifier with hybrid pulse modulation. , 2015, , .		9
100	12.9 A flying-domain DC-DC converter powering a Cortex-M0 processor with 90.8% efficiency. , 2016, , .		9
101	A 78 pW 1 b/s 2.4 GHz radio transmitter for near-zero-power sensing applications. , 2013, , .		8
102	A 1.65 mW PLL-free PSK receiver employing super-regenerative phase sampling. , 2015, , .		8
103	Flying-Domain DC–DC Power Conversion. IEEE Journal of Solid-State Circuits, 2016, 51, 2830-2842.	5.4	8
104	A sub-1.55mV-accuracy 36.9ps-FOM digital-low-dropout regulator employing switched-capacitor resistance. , 2018, , .		8
105	A 113 pW fully integrated CMOS temperature sensor operating at 0.5 V. , 2017, , .		7
106	A 0.3V biofuel-cell-powered glucose/lactate biosensing system employing a 180nW 64dB SNR passive Î'Ï, ADC and a 920MHz wireless transmitter. , 2018, , .		7
107	17.6 A Sub-40μW 5Mb/s Magnetic Human Body Communication Transceiver Demonstrating Trans-Body Delivery of High-Fidelity Audio to a Wearable In-Ear Headphone. , 2019, , .		7
108	Low-power integrated circuits for wearable electrophysiology. , 2021, , 163-199.		7

7

#	ARTICLE	IF	CITATIONS
109	A 94.2-dB SNDR 142.6-μW VCO-Based Audio ADC With a Split-ADC Differential Pulse Code Modulation Architecture. IEEE Solid-State Circuits Letters, 2021, 4, 121-124.	2.0	7
110	A Novel Ultrafast Transient Constant on-Time Buck Converter for Multiphase Operation. IEEE Transactions on Power Electronics, 2021, 36, 13096-13106.	7.9	7
111	Multi-channel 180pJ/b 2.4GHz FBAR-based receiver. , 2012, , .		6
112	Narrowband Transmitters: Ultralow-Power Design. IEEE Microwave Magazine, 2015, 16, 130-142.	0.8	6
113	A single-inductor 7+7 ratio reconfigurable resonant switched-capacitor DC-DC converter with 0.1-to-1.5V output voltage range. , 2015, , .		6
114	A Recursive Switched-Capacitor House-of-Cards Power Amplifier. IEEE Journal of Solid-State Circuits, 2017, 52, 1719-1738.	5.4	6
115	A 678- <inline-formula> <tex-math notation="LaTeX">\$mu\$ </tex-math> </inline-formula> W Frequency-Modulation-Based ADC With 104-dB Dynamic Range in 44-kHz Bandwidth. IEEE Transactions on Circuits and Systems II: Express Briefs, 2018, 65, 1370-1374.	3.0	6
116	A Charge-Pump-based Digital LDO Employing an AC-Coupled High-Z Feedback Loop Towards a sub-4fs FoM and a 105,000x Stable Dynamic Current Range. , 2019, , .		6
117	An interdigitated non-contact ECG electrode for impedance compensation and signal restoration. , 2015, , .		5
118	A footprint-constrained efficiency roadmap for on-chip switched-capacitor DC-DC converters. , 2015, ,		5
119	26.4 A 0.4-to-1V 1MHz-to-2GHz switched-capacitor adiabatic clock driver achieving 55.6% clock power reduction. , 2017, , .		5
120	A 5.5 nW battery-powered wireless ion sensing system. , 2017, , .		5
121	AMASS PLL: An Active-Mixer-Adopted Sub-Sampling PLL Achieving an FOM of â^255.5DB and a Reference Spur of â^266.6DBC. , 2018, , .		5
122	Bell–Bloom Magnetometer Linearization by Intensity Modulation Cancellation. IEEE Transactions on Instrumentation and Measurement, 2020, 69, 883-892.	4.7	5
123	20.1 A 28ÂμW IoT Tag That Can Communicate with Commodity WiFi Transceivers via a Single-Side-Band QPSK Backscatter Communication Technique. , 2020, , .		5
124	A â^'254.1-dB FoM 2.4-GHz Subsampling PLL With a â^'76-dBc Reference Spur by Employing a Varactor-Based Cancellation Technique. IEEE Solid-State Circuits Letters, 2020, 3, 102-105.	2.0	5
125	Investigating well potential parameters on neural spike enhancement in a stochastic-resonance pre-emphasis algorithm. Journal of Neural Engineering, 2021, 18, 046062.	3.5	5
126	A 110µW 10Mb/s etextiles transceiver for body area networks with remote battery power. , 2010, , .		4

#	Article	IF	CITATIONS
127	A 78%-efficiency li-ion-compatible fully-integrated modified 4-level converter with 0.01–40mW DCM-operation in 28nm FDSOI. , 2018, , .		4
128	A â^'105dB THD 88dB-SNDR VCO-Based Sensor Front-End Enabled by Background-Calibrated Differential Pulse Code Modulation. , 2020, , .		4
129	Maximizing Wireless Power Transfer to Intraocular Implants Under Unconstrained Eye Movements. , 2021, , .		4
130	A 3.75 nW Analog Electrocardiogram Processor Facilitating Stochastic Resonance for Real-Time R-wave Detection. , 2021, , .		4
131	A 440pJ/bit 1Mb/s 2.4GHz multi-channel FBAR-based TX and an integrated pulse-shaping PA. , 2012, , .		3
132	A multi-channel EEG system featuring single-wire data aggregation via FM-FDM techniques. , 2016, , .		3
133	22.2 A Rugged Wearable Modular ExG Platform Employing a Distributed Scalable Multi-Channel FM-ADC Achieving 101dB Input Dynamic Range and Motion-Artifact Resilience. , 2019, , .		3
134	17.5 A 98.2%-Efficiency Reciprocal Direct Charge Recycling Inductor-First DC-DC Converter. , 2021, , .		3
135	A Battery-Connected Symmetric Modified Multilevel Ladder Converter Achieving 0.45W/mm2 Power Density and 90% Peak Efficiency. , 2019, , .		2
136	A Battery-Connected Inductor-First Flying Capacitor Multilevel Converter Achieving 0.77W/mm ² and 97.1% Peak Efficiency. , 2021, , .		2
137	Pulsed Ultra-Wideband Transceivers. Integrated Circuits and Systems, 2015, , 233-280.	0.2	2
138	Enabling Sub-nW RF circuits through subthreshold leakage management. , 2013, , .		1
139	Introduction to Ultra Low Power Transceiver Design. Integrated Circuits and Systems, 2015, , 1-23.	0.2	1
140	A recursive house-of-cards digital power amplifier employing a λ/4-less Doherty power combiner in 65nm CMOS. , 2016, , .		1
141	Power Management for the Internet of Things. , 2019, , .		1
142	Wireless data communication for ECoG implants. , 2019, , 145-169.		1
143	Guest Editorial—Selected Papers from the 2013 IEEE International Solid-State Circuits Conference (ISSCC). IEEE Transactions on Biomedical Circuits and Systems, 2013, 7, 733-734.	4.0	0
144	Guest Editorial—Selected Papers from the 2014 IEEE International Solid-State Circuits Conference. IEEE Transactions on Biomedical Circuits and Systems, 2014, 8, 753-754.	4.0	0

#	Article	IF	CITATIONS
145	Architectures for Ultra-Low-Power Multi-Channel Resonator-Based Wireless Transceivers. Integrated Circuits and Systems, 2015, , 97-135.	0.2	0
146	Introduction to the Special Issue on the 2018 IEEE International Solid-State Circuits Conference (ISSCC). IEEE Journal of Solid-State Circuits, 2018, 53, 3015-3016.	5.4	0
147	RF power transmission and its considerations for ECoG implants. , 2019, , 121-144.		0
148	ECoG signal coding and digitization. , 2019, , 51-71.		0
149	Integrated circuit interfaces for electrocortical stimulation. , 2019, , 73-96.		0
150	Power management for mm-sized ECoG implants. , 2019, , 97-119.		0
151	Introduction to ECoG interfaces. , 2019, , 1-30.		0
152	A GMSK/PAM4 Multichannel Magnetic Human Body Communication Transceiver. IEEE Solid-State Circuits Letters, 2022, 5, 66-69.	2.0	0
153	A 900MHz GFSK and 16-FSK TX Achieving Up to 63.9% TX Efficiency and 76.2% PA Efficiency via a DC-DC-Powered Class-D VCO and a Class-E PA. IEEE Transactions on Circuits and Systems II: Express Briefs, 2022, 69, 3739-3743.	3.0	0
154	Analysis and Measurement of Noise Suppression in a Nonlinear Regenerative Amplifier. IEEE Transactions on Circuits and Systems I: Regular Papers, 2022, 69, 4117-4127.	5.4	0

Transactions on Circuits and Systems I: Regular Papers, 2022, 69, 4117-4127. 154